Progress In Electromagnetics Research, Vol. 124, 55–70, 2012

A NOVEL WIDEBAND ANTENNA ARRAY WITH TIGHTLY COUPLED OCTAGONAL RING ELEMENTS

Y. Chen, S. Yang*, and Z. Nie

School of Electronic Engineering, University of Electronic Science and Technology of China (UESTC), Chengdu 611731, China

Abstract—A novel phased array antenna with wide bandwidth and wide scan angle is presented. The radiating aperture of the phased array consists of periodically and closely spaced octagonal ring elements. Tight capacitive coupling between adjacent elements is realized by interdigitating the end portions of the ring elements. To improve the impedance matching of the individual antenna elements over wide frequency band, a novel impedance matching layer consists of periodic octagonal ring element is subtly designed and placed over the radiating aperture. Both of the radiating elements and impedance matching layer are printed on a flexible membrane substrate with a thickness of 0.04 mm. Measured results of a 16-element linear array demonstrate that good impedance matching over a 4.4 : 1 bandwidth can be obtained for beam scan angles within $\pm 45^\circ$ from broadside. As compared to conventional wideband phased array such as tapered slot antenna array, the proposed phased array has the features such as low cost, low profile, light weight, and ease of fabrication.

1. INTRODUCTION

Phased array antenna systems play a major role in defense as well as in commercial applications [1–5]. As broadband and multifunction electronic systems become more widespread in commercial and military applications, the interest and need for developing phased array antennas with multi-octave operating bandwidth and wide scan angle is increased [6–10]. Therefore, the problem of designing a phased array with good impedance matching and excellent scanning property over a wide frequency band is becoming an important topic in modern antenna array community.

Received 13 December 2011, Accepted 4 January 2012, Scheduled 11 January 2012

* Corresponding author: Shiwen Yang (swnyang@uestc.edu.cn).

Although wideband phased array design is a long-standing topic of interest, progress has recently been made using endfire tapered slot antennas. The stripline fed tapered slot antenna, often called Vivaldi antenna, was firstly introduced by Lewis et al. in 1974, and later was often employed as the antenna element to build up wideband phased array antennas [11–13]. The Vivaldi antenna is a member of the class of continuously scaled, gradually curved, and slows leaky endfire travelling wave antennas. Different parts of the antenna radiate at different frequencies, while the size of the radiating part is constant in wavelength. Thus, the Vivaldi antenna has theoretically unlimited operating frequency range. Practically, the operating bandwidth is limited by the transition from the feeding transmission line to the slot line of the antenna, and by the finite dimensions of the antenna [14]. Generally, the tapered slot is greater than one-half wavelength at the low end of the band, and more than two wavelengths at the high end for a $3:1$ bandwidth [15].

On the other hand, the compactness of a phased array is another important issue in modern electronic systems, especially in satellite communication systems, where the cost for launch per kilogram of mass is comparable to the cost for the satellite development itself [15]. Short tapered slot antenna are essential for achieving compactness or low profile configurations, but they inevitably suffer from high voltage standing wave ratio (VSWR), due to the impedance mismatch at the feeding and terminating ends. To alleviate the stringent low profile configuration in many applications, an alternative flared dipole, also known as bunny ear antenna, was used to form an egg-crate dual-polarized array [16]. This element is much shorter than the classic Vivaldi antenna, and it has a lower cutoff frequency, made possible by etching out the conducting area near the feed points. However, the profile height of bunny ear antenna is still far from the low profile and conformal characteristics that can be realized by microstrip antennas [17, 18]. Additionally, wideband phased arrays developed from such tapered slot antenna elements should be compact enough to allow sufficiently small element spacing to allow grating lobe free scanning at the high frequency end. However, due to the strong mutual coupling between antenna elements, performances of elements in array environment differ greatly from those of isolated Vivaldi antennas. Furthermore, the general continuous metal plate structure in Vivaldi antenna arrays may induce higher order modes along the E-plane [19]. To suppress these modes, thick elements are usually accepted to reduce the gap and shift the cutoff frequency out of the band. This, however, makes it difficult to form a dual-polarized aperture. Apparently, antenna arrays based on wideband tapered slot

antenna element cannot well meet stringent requirements such as low profile, platform conformable and wide bandwidth simultaneously.

In recent years, a fundamentally different approach to broadband array design has been developed [7, 20–26]. The exemplified antenna arrays based on such novel methodology serve as the practical implementations of Wheeler's theoretical "current sheet array" (CSA) concept [27]. The methodology of forming broadband arrays from tightly-coupled, electrically small elements has been proven by several researchers. They found that the novel methodology is applicable to arrays with dipole elements, pixelated elements, and long slot array. Specifically, Munk [7] demonstrated that dipole arrays with strong mutual coupling can operate over much larger bandwidth than that of an individual dipole element. This type of tightly coupled dipole array was further demonstrated, which was found that the impedance stability over wide frequency band and the maximum scan angle from broadside can be further enhanced by placing properly designed dielectric layers on top of the dipole array aperture. The results of this groundbreaking development represent the current state of the art in broadband array design. Based on the same methodology, Georgia Technology Research Corporation developed a broadband fragmented aperture antenna array with periodic pixelated elements [23]. Each pixelated element has a periphery that extends into the area of its adjacent element, such that a connected array is formed and strong mutual coupling is introduced between adjacent elements. The locations of the conducting parts in pixelated elements are determined by a multistage optimization procedure that continuously tailors the performance of the array. Measured results have shown that a $33:1$ bandwidth can be realized by the fragmented aperture antenna array, and it is claimed that a $100:1$ bandwidth can be obtained by further optimizing the configuration of the pixelated elements [23]. As another promising approach to wideband phased array design, the wideband low profile phased array using long slot aperture is also a practical implementation of Wheeler's current sheet array [24–26]. A prototype UHF array with 4×8 elements was built and fabricated by Lee et al. [28]. The measured results of a prototype UHF array demonstrated that at least a $4:1$ bandwidth can be obtained by such long slot antenna array.

The design presented in this paper is another practical implementation of Wheeler's current sheet array, which differs from the aforementioned designs. As compared to the simple electronic dipole elements in Munk's CSA [7] or magnetic dipole elements in Lee's long slot array [24], the new CSA design allows a compact and convenient feed structure design for the integration of dual

polarization. Furthermore, the metal layer placed above the radiating aperture, working as a wide angle impedance matching (WAIM) layer, is used to compensate the impedance mismatch caused by beam scanning. Another benefit from the new WAIM layer is that it will reduce the loss occurred in conventional WAIM, which is usually made up of multilayer of dielectric slabs. Therefore, the gain performance of the new CSA design is improved and the overall height of the array is reduced. Both of the radiating elements and the new WAIM are printed on a flexible membrane substrate with a thickness of 0.04 mm and a dielectric constant of $\varepsilon_r = 2.2$. Expanded polystyrene foam is used to fill the space between the radiating aperture and the reflecting ground, and between the radiating aperture and the new WAIM layer. Thus, the present design is low cost, low profile, light weight, and easy to be fabricated. Although the shape of the antenna element is similar to that has been published by Yongwei Zhang in Octorber 2011 [29], the operating bandwidth, feed structure, and array structure are quite different. In order to remove any concern of plagiarism, it is necessary to point out that the antenna array presented here was independently developed by us, the research work on this antenna includes the analysis, design, and measurement was finished in December 2010.

2. DESIGN AND CHARACTERIZATIONS OF THE RING ELEMENT IN INFINITE ARRAY

This section presents the geometry and characterizations of an octagonal ring element in an infinite array environment. Figure 1

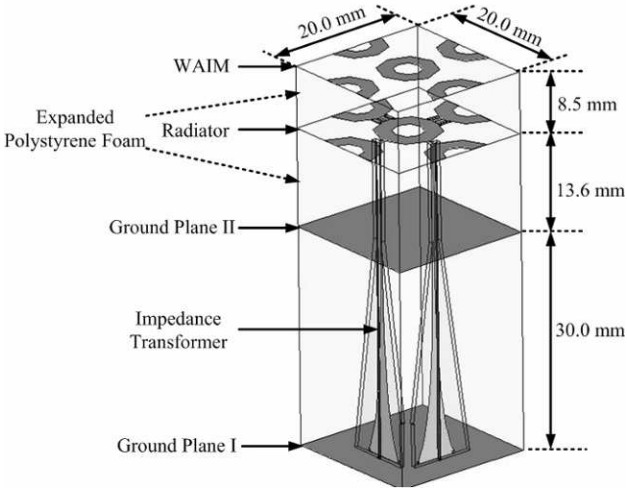

Figure 1. Unit cell geometry of the octagonal ring antenna array.

shows the unit cell of the octagonal ring element antenna, which is composed of the radiator element, WAIM element, impedance transformer structure, and two ground planes. The spacing between adjacent elements is 20.0 mm, which is slightly greater than half wavelength at the highest frequency (9.0 GHz for the unit cell) and is usually adopted by most conventional endfire tapered slot antenna array. The distance from the radiator layer to ground plane II is 13.6 mm, which is about one quarter wavelength at the center frequency of the operating frequency band. The distance from the WAIM layer to the radiator layer is jointly optimized with the shape of the WAIM unit cell using the commercial software Ansoft HFSS [30]. The space between the radiator and ground plane I, and the space between the radiator and WAIM layer are both filled with expanded polystyrene foam.

The shape of the unit cell for the radiator and WAIM layer is shown in Figure 2. To lower the array's operating frequency in such kind of tightly coupled arrays, larger capacitance is usually introduced at the tip of each element. In Figure 2(a), it has been shown that interdigitated capacitors were employed and accordingly the mutual capacitance dominates for this tightly coupled octagonal ring antenna array. For the dual-polarized phased array, capacitors of 5 pF are needed. The interdigitated capacitor can be built with 5 fingers with finger length $L_{\text{finger}} = 1.4$ mm and finger width $W_{\text{finger}} = 0.3$ mm. The gap between adjacent fingers is $G_{\text{finger}} = 0.35$ mm. Other design parameters are also listed in Figure 2(a). As shown in Figure 2(b),

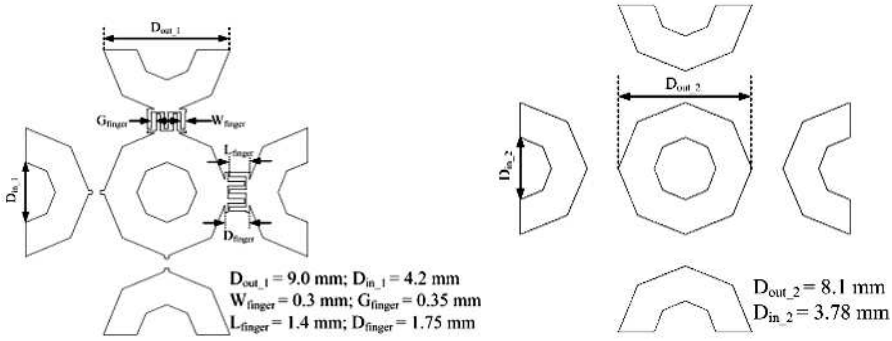

Figure 2. Configurations of the radiator and WAIM element with octagonal ring shapes. (a) Unit cell configuration of the octagonal ring element in the radiator layer. (b) Unit cell configuration of the octagonal ring element in the WAIM layer.

the unit cell of the octagonal ring element for the WAIM layer is just a scaled down version of that in the radiator layer, i.e., the octagonal ring element in the WAIM layer follows the same pattern as that in the radiator layer, but with a smaller size. The Ansoft HFSS software is used to optimize the physical dimensions for the radiator and WAIM layer. The optimization shows that the bandwidth performance of the periodic array is sensitive to $D_{\text{out\_1}}$, $D_{\text{in\_1}}$, and the scale factor for the WAIM layer. In our optimization procedure, the scale factor is first fixed, and we perform parameter sweeps for $D_{\text{out\_1}}$, $D_{\text{in\_1}}$. Once the optimal $D_{\text{out\_1}}$, $D_{\text{in\_1}}$ is obtained, a parameter sweep is carried out for the scale factor. As compared with the tightly coupled dipole array proposed by Munk et al. the octagonal ring element shown in Figure 2(a) is more suitable for the integration of dual polarization. This benefit is mainly due to the separation of the feed ports for the two different polarizations. Both of the radiator and the WAIM are printed on a membrane substrate with a thin thickness of 0.04 mm and a relative permittivity of 2.6.

The impedance transformer shown in Figure 3 was also optimized by iteration to achieve a good impedance match, in which the microstrip line is transformed into a pair of 110 Ω parallel lines, and finally exciting the octagonal ring antenna element. The impedance transformer optimization is also performed using the Ansoft HFSS software. The objective of this optimization is to reduce the VSWR values over the operating frequency band of the antenna array. As compared to the optimization process for the unit cell, the impedance transformer optimization is relatively simple, in which only the exponential term in the equation presented in Figure 3 is swept, and we found that when the exponential term equals to 0.18, a lowest average VSWR over the frequency band can be achieved. The microstrip line was designed to match a 50 Ω input SMA connector. The distance

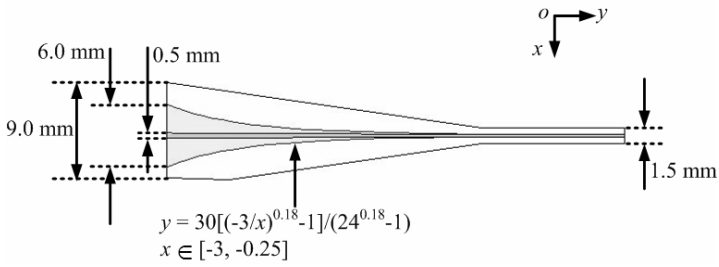

Figure 3. Dimensions of the impedance transformer in the unit cell of an octagonal ring element array.

between ground plane I and ground plane II is 30.0 mm, which is just the length of the tapered section in the impedance transformer. The impedance transformer shown in Figure 3 is printed on a 0.635 mm thick Rogers 5880 substrate ($\varepsilon_r = 2.2$). The specific design parameters and dimensions shown in Figure 3 are the preferred design dimensions, which is the result of the optimization design. Although the height of the transformer is relatively higher as compared to the size of the radiator, it is a low cost design. For applications where the profile height is very strict, other designs such as co-planar balun embedded in a circuit board behind the ground plane can be used. The impedance transformers as well as the structures over ground plane II are fixed by foam spacers.

Figure 4 shows the simulated excited surface currents over the unit cell radiator at 2.5 GHz, 4.0 GHz, 6.0 GHz, and 8.5 GHz, respectively. The simulated results are obtained using Ansoft HFSS. The behavior at these selected frequencies can well illustrate the performance of the

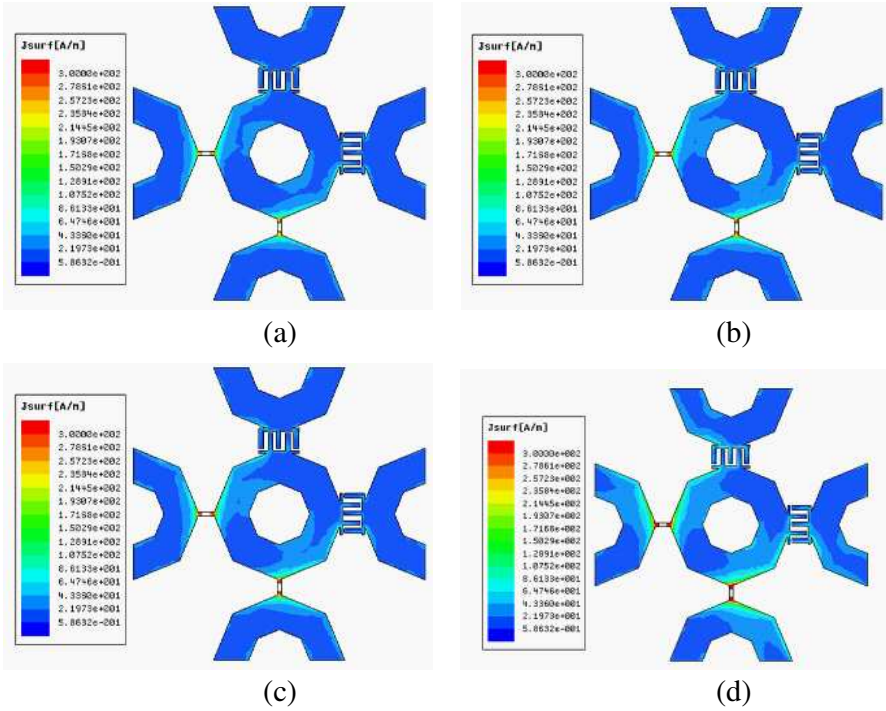

Figure 4. Surface current distribution on the octagonal ring element in an infinite array environment. (a) 2.5 GHz. (b) 4.0 GHz. (c) 6.0 GHz. (d) 8.5 GHz.

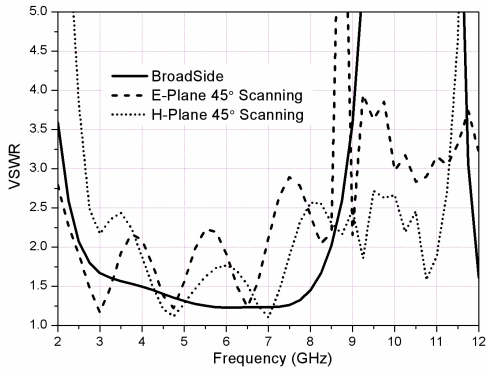

Figure 5. Active input VSWR calculated by HFSS over unit cell of the octagonal ring element antenna.

infinite octagonal ring element array over the wide frequency band. As can be seen, the surface current distributions are rather stable at the four frequencies, which illustrates that the performance of the infinite octagonal ring element array varies slowly with the frequency. This fact further implies that this array should have stable radiation characteristics and impedance characteristics over a wide frequency band. The broadside as well as the scanning active VSWRs of an infinite dual-polarized octagonal ring element array was calculated by using HFSS over a unit cell. The VSWR performance shown in Figure 5 suggests that satisfactory scanning properties and wideband performance could be achieved over a $4.5:1$ frequency band.

3. DESIGN OF THE SINGLE POLARIZED FINITE ARRAY

In order to demonstrate the functionality of a phased array built from the basic octagonal ring element we have described, a prototype consisting of 24×3 elements was fabricated. Figure 6 shows the perspective view of the wideband antenna array with tightly coupled octagonal ring elements, and the physical dimensions of the unit cell elements are kept the same as those shown in Figures 1–3. As can be seen, only the 16 elements located at the center of the array are actively excited through the impedance transformers. It indicates that all the other elements surrounding the central elements serve as the dummy elements, which provide a uniform infinite array environment to the actively excited elements. Therefore, the phased array given in Figure 6 is actually a 1×16 dual-polarized phased array.

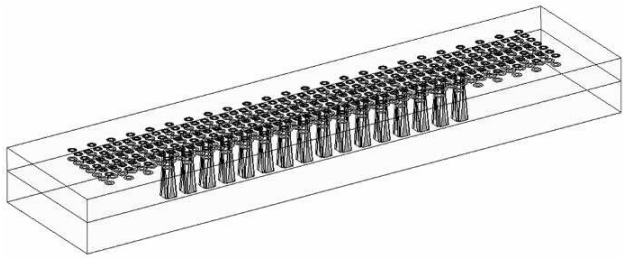

Figure 6. The perspective view of the wideband antenna array with tightly coupled octagonal ring elements.

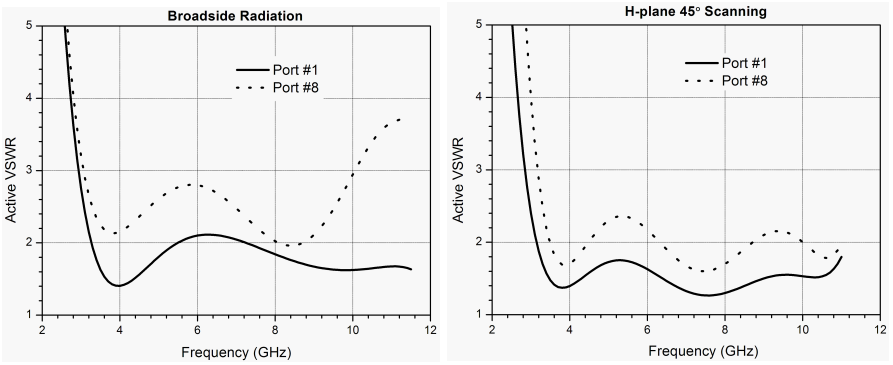

(a) (b)

Figure 7. Simulated VSWR performance for a 1×16 finite array. (a) Broadside radiation. (b) 45° scanning in the H-plane.

The design goal herein is to achieve wide bandwidth and wide scanning angle for 2.5–11.0 GHz applications. The typical simulated VSWR performances for elements located at the edge of the array (port #1) and at the center of the array (port #8) are shown in Figure 7. From the simulation results it can be seen that the proposed antenna has a 4.4 : 1 bandwidth for both of the broadside radiation and H-plane 45° scanning.

The array was manufactured using existing printed circuit technology to show its producibility. As compared to conventional wideband phased array such as tapered slot antenna array, we found that the proposed phased array is low cost, light weight, and much easier to fabricate. Figure 8 shows the photograph of the fabricated 1×16 octagonal ring antenna array in the H-plane. As can be seen, a 16-way corporate feed network consisting of commercial power dividers and microwave coax was employed to feed the array. This

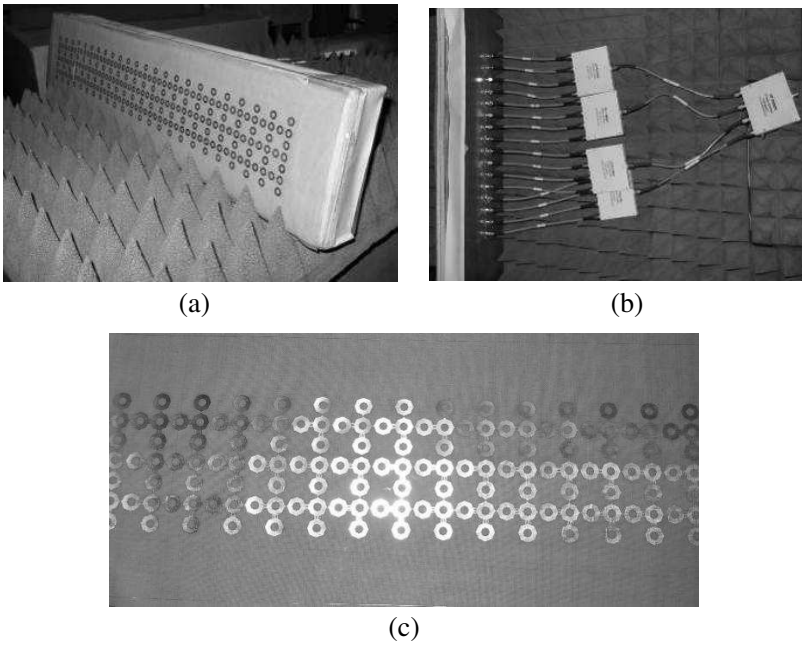

Figure 8. Photographs of the prototype 1×16 octagonal ring antenna array. (a) Front view of the fabricated antenna array. (b) 16-way corporate feed network consisting of commercial power dividers and microwave coax. (c) Photograph of the fabricated radiator layer.

scheme is extensively employed in antenna array systems such as mobile communication systems [31–34]. Since the radiator layer is embedded under the WAIM layer and thus invisible in Figure 8(a), we present the photograph of the fabricated radiator layer in Figure 8(c).

In order to protect the array, a thin dielectric sheet can be placed on top of the WAIM layer without affecting the array characteristics significantly. The four sides of the array can be left open or sealed with absorbing material. It is worthy to note that there is no blind angle observed in the experiment or HFSS simulations, within the desired scanning ranges.

4. EXPERIMENTAL RESULTS

In the experiment, all the dummy elements were terminated with $110\,\Omega$ resistors while the central 16 elements were actively excited (only for one polarization) for measurement. Radiation patterns and gain were measured in a far-field antenna measurement system [35], with a maximum far-field distance of 15.0 meters. Considering the physical

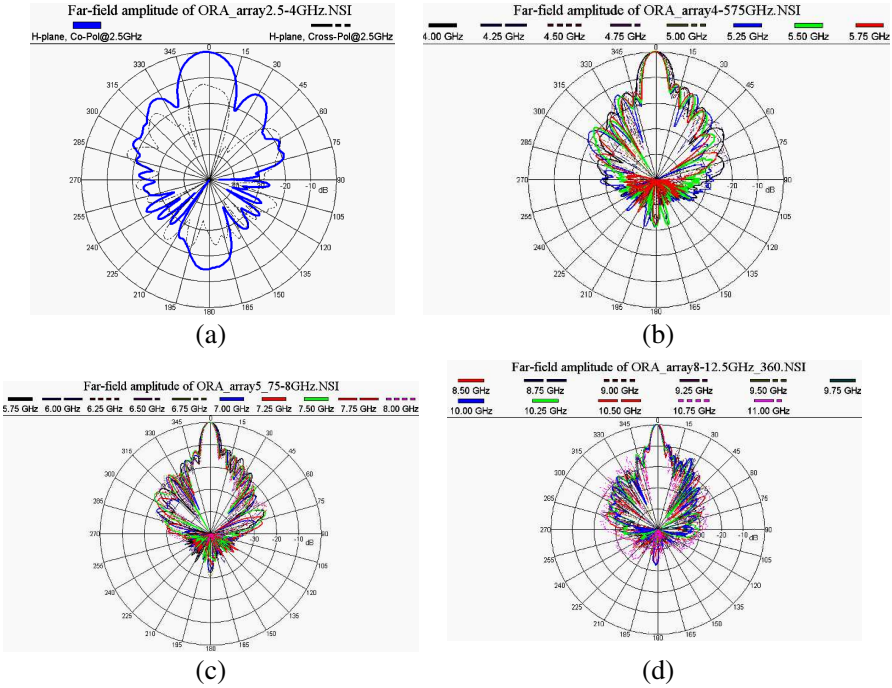

Figure 9. Measured and normalized array pattern in the broadside radiation case. (a) 2.5 GHz. (b) 4.0–5.75 GHz. (c) 5.75–8.0 GHz. (d) 8.5–11.0 GHz.

dimensions and operating frequency band of the current phased array, the far-field range is suitable for the accurate measurement of radiation patterns and gains. Since the phased array designed has wider bandwidth than conventional antennas or antenna arrays, a group of narrow band open-ended waveguide probes were used to illuminate the test array for each narrow frequency band. Similarly, a group of narrow band standard gain horn antennas were employed for the realized gain measurement of the 1×16 octagonal ring antenna array.

The measured normalized array patterns at typical operating frequencies for the broadside radiation case, 30° and 45° scanning cases are plotted in Figures 9, 10, and 11, respectively. The scanning cases were measured by using two sets of cables (served as the delay lines) and were trimmed for the 30° and 45° beam scan angles, respectively. These patterns show beam scanning capabilities to large angles from broadside over a wide frequency band. Moreover, it is found that the measured main beam directions agree well with the desired directions of 30° and 45°.

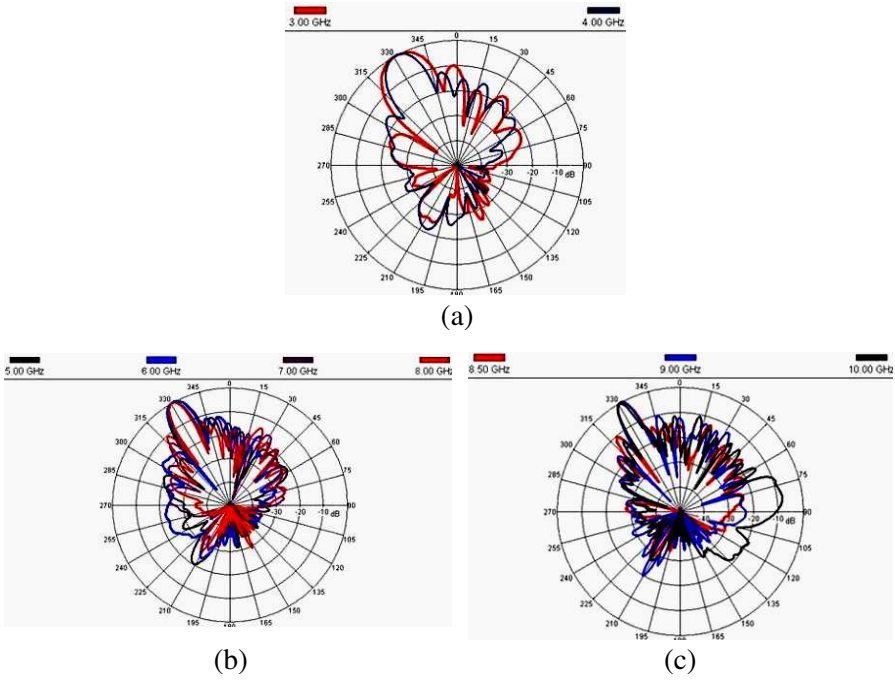

Figure 10. Measured and normalized array pattern in the 30° scanning case. (a) 3.0–4.0 GHz. (b) 5.0–8.0 GHz. (c) 8.5–10.0 GHz.

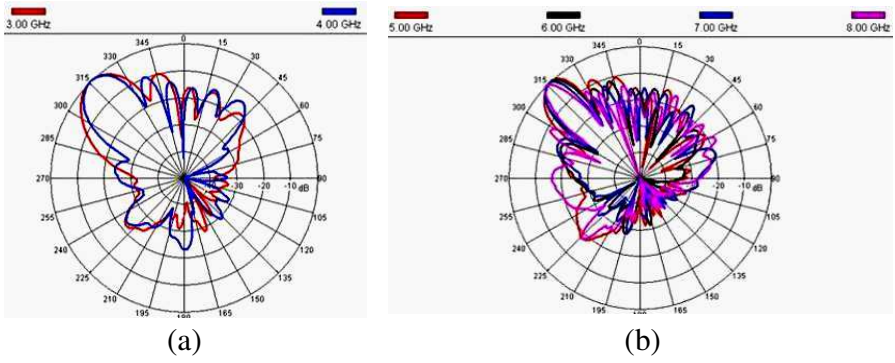

Figure 11. Measured and normalized array pattern in the 45° scanning case. (a) 3.0–4.0 GHz. (b) 5.0–8.0 GHz.

Figure 12 shows the realized gain of the octagonal ring phased array with the feed loss removed for the broadside radiation. The curve for the theoretical directivity (virtual area gain) is also included for reference. It is reasonable to conclude that the drop gain at higher

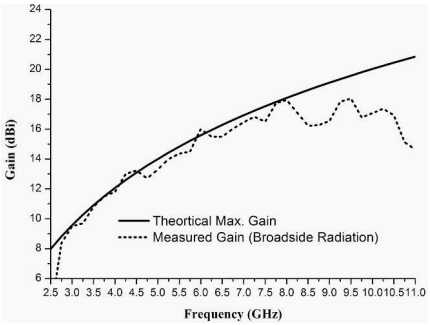

Figure 12. Measured gain of the octagonal ring phased array in the broadside radiation case (without the feed loss).

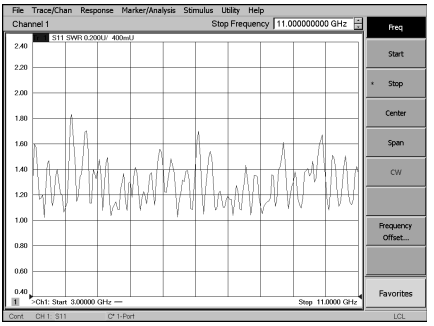

Figure 13. Measured VSWR performance for the 1×16 octagonal ring phased array.

frequencies is due to the common-mode resonance occurring in the long vertical feeding line [36]. Nonetheless, the 1×16 octagonal ring phased array is considered to be well behaved in that the gain tracks fairly well with the theoretical values defined by the maximum capture area of the antenna array. The gain ripples are attributed to the imperfections of the setup and residual mismatch of the input feed port. Also, there is some uncertainty in the calibration of feed loss and gain horn. Apparently, for an active array, with each element supported by a T/R module, the receiving loss will be limited by the low noise amplifier, thus further improving the gain efficiency. The performance demonstrated so far shows great potential of the octagonal ring phased array for many wideband applications.

Since the 16-way corporate feed network is necessary to be employed to feed the octagonal ring phased array, the VSWR performance is measured at the primary input port of the feed network. As shown in Figure 13, the array was well matched over the operating frequency band, with a maximum VSWR value of 1.82.

5. CONCLUSION

A novel wideband phased array with tightly coupled octagonal ring elements was proposed and designed, and a practical prototype phased array was fabricated and measured. Good performance was observed. From the fabricated phased array, the measured results showed that good impedance match and radiation performance over a 4.4 : 1 bandwidth can be obtained for arrays scanned within $\pm 45^\circ$ from broadside. Since the novel array element configuration permits

the low profile and compact design of a wideband dual-polarized phased array, its technical outcome could be utilized as a core infrastructure technology for many wideband applications in the future.

ACKNOWLEDGMENT

This work was supported by the Natural Science Foundation of China under Grant Nos. 60971030, 61125104.

REFERENCES

1. Yngvesson, K. S., D. H. Schaubert, T. L. Korzeniowski, E. L. Kollberg, T. Thungren, and J. F. Johansson, "Endfire tapered slot antennas on dielectric substrates," *IEEE Trans. Antennas Propagat.*, Vol. 33, No. 12, 1392–1399, 1985.
2. Xu, Z., Y. Yuan, X. Q. Yan, Z. H. Feng, and Q. Z. Liu, "Scan blindness of tapered-slot array optimized with tapered-aerosubstrate in the triangular elements grids," *Journal of Electromagnetic Waves and Applications*, Vol. 25, No. 8–9, 1329–1339, 2011.
3. Hansen, R. C., *Phased Array Antennas*, John Wiley & Sons, Inc., New York, 1998.
4. Liao, W.-J., S.-H. Chang, and W.-H. Lee, "Beam scanning array using spatial diversity," *Journal of Electromagnetic Waves and Applications*, Vol. 25, No. 4, 481–494, 2011.
5. Mailloux, R. J., *Phased Array Antenna Handbook*, Artech House, Inc., Norwood, 2005.
6. Holter, H., T. H. Chio, and D. H. Schaubert, "Experimental results of 144-element dual-polarized endfire tapered-slot phased arrays," *IEEE Trans. Antennas Propagat.*, Vol. 48, No. 11, 1707–1718, 2000.
7. Munk, B. A., et al., "A low-profile broadband phased array antenna," *Proc. Antennas Propagation Soc. Int. Symp.*, 448–451, Columbus, OH, Jun. 2003.
8. Oikonomou, A., I. S. Karanasiou, and N. K. Uzunoglu, "Phased-array near field radiometry for brain intracranial applications," *Progress In Electromagnetics Research*, Vol. 109, 345–360, 2010.
9. Eldek, A. A., A. Z. Elsherbeni, and C. E. Smith, "Rectangular slot antenna with patch stub for ultra wideband applications and phased array systems," *Progress In Electromagnetics Research*, Vol. 53, 227–237, 2005.

10. Eldek, A. A., "Design of double dipole antenna with enhanced usable bandwidth for wideband phased array applications," *Progress In Electromagnetics Research*, Vol. 59, 1–15, 2006.
11. Lewis, L. R., M. Fasset, and J. Hunt, "A broadband stripline array element," *IEEE Symp. Antennas and Propagation Dig.*, 335–337, Atlanta, GA, 1974.
12. Zhou, B., H. Li, X. Zou, and T.-J. Cui, "Broadband and high-gain planar vivaldi antennas based on inhomogeneous anisotropic zero-index metamaterials," *Progress In Electromagnetics Research*, Vol. 120, 235–247, 2011.
13. Yang, Y., Y. Wang, and A. E. Fathy, "Design of compact Vivaldi antenna arrays for UWB see through wall applications," *Progress In Electromagnetics Research*, Vol. 82, 401–418, 2008.
14. Shin, J. and D. H. Schaubert, "A parameter study of stripline-fed Vivaldi notch-antenna arrays," *IEEE Trans. Antennas Propagat.*, Vol. 47, No. 5, 879–886, 1999.
15. Lee, J. J., S. Livingston, and R. Koenig, "A low-profile wide-band (5 : 1) dual-pol array," *IEEE Antennas Wireless Propag. Lett.*, Vol. 2, 46–49, 2003.
16. Li, X., Y.-J. Yang, X. Tao, L. Yang, S.-X. Gong, Y. Gao, K. Ma, and X.-L. Liu, "A novel design of wideband circular polarization antenna array with high gain characteristic," *Journal of Electromagnetic Waves and Applications*, Vol. 24, No. 7, 951–958, 2010.
17. Wong, K., *Compact and Broadband Microstrip Antennas*, John Wiley & Sons, Inc., New York, 2002.
18. Chen, Y., S. Yang, and Z. Nie, "Bandwidth enhancement method for low profile E-shaped microstrip patch antennas," *IEEE Trans. Antennas Propagat.*, Vol. 58, No. 7, 2442–2447, 2010.
19. Schaubert, D. H., "A class of E-plane scan blindnesses in single-polarized arrays of tapered-slot antennas with a ground plane," *IEEE Trans. Antennas Propagat.*, Vol. 44, No. 7, 954–959, 1996.
20. Munk, B. A., *Finite Antenna Arrays and FSS*, Wiley, New York, 2003.
21. Hansen, R. C., "Current induced on a wire: Implications for connected arrays," *IEEE Antennas Wireless Propag. Lett.*, Vol. 2, 288–289, 2003.
22. Hansen, R. C., "Linear connected arrays," *IEEE Antennas Wireless Propag. Lett.*, Vol. 3, 154–156, 2004.
23. Georgia Technology Research Corporation, [Online]. Available: http://www.gtri.gatech.edu/casestudy/100-1-bandwidth.

24. Lee, J. J., S. Livingston, and R. Koenig, "Wide band long slot array antennas," *Proc. Antennas Propagation Soc. Int. Symp.*, 452–455, Columbus, OH, 2003.
25. Neto, A. and J. J. Lee, "Infinite bandwidth long slot array antenna," *IEEE Antennas Wireless Propag. Lett.*, Vol. 4, 75–78, 2005.
26. Neto, A. and J. J. Lee, "Ultrawide-band properties of long slot arrays," *IEEE Trans. Antennas Propagat.*, Vol. 54, No. 2, 534–543, 2006.
27. Wheeler, H. A., "Simple relations derived from a phased array antenna made of an infinite current sheet," *IEEE Trans. Antennas Propagat.*, Vol. 13, No. 4, 506–514, 1965.
28. Lee, J. J., S. Livingston, R. Koenig, D. Nagata, and L. L. Lai, "Compact light weight UHF arrays using long slot apertures," *IEEE Trans. Antennas Propagat.*, Vol. 54, No. 7, 2009–2015, 2006.
29. Zhang, Y. and K. B. Anthony, "Octagonal ring antenna for a compact dual-polarized aperture array," *IEEE Trans. Antennas Propagat.*, Vol. 59, No. 10, 3927–3932, 2011.
30. Ansoft Corporation HFSS, [Online]. Available: http://www.ansoft.com /products/hf/hfss/.
31. Zhang, H., X.-W. Shi, F. Wei, and L. Xu, "Compact wideband GYSEL power divider with arbitrary power division based on patch type structure," *Progress In Electromagnetics Research*, Vol. 119, 395–406, 2011.
32. Lin, Z. and Q.-X. Chu, "A novel approach to the design of dual-band power divider with variable power dividing ratio based on coupled-lines," *Progress In Electromagnetics Research*, Vol. 103, 271–284, 2010.
33. Wu, Y., Y. Liu, S. Li, C. Yu, and X. Liu, "Closed-form design method of an N-way dual-band wilkinson hybrid power divider," *Progress In Electromagnetics Research*, Vol. 101, 97–114, 2010.
34. Al-Zayed, A. S. and S. F. Mahmoud, "Seven ports power divider with various power division ratios," *Progress In Electromagnetics Research*, Vol. 114, 383–393, 2011.
35. Nearfield Systems Inc., [Online]. Available: http://www.nearfield.com.
36. Cavallo, D., A. Neto, and G. Gerini, "PCB slot based transformers to avoid common-mode resonances in connected arrays of dipoles," *IEEE Trans. Antennas Propagat.*, Vol. 58, No. 8, 2767–2771, 2010.